Composites Communications 12 (2019) 86–90

Contents lists available at ScienceDirect

Composites Communications

journal homepage: www.elsevier.com/locate/coco

Toughening an epoxy network by the addition of an acrylic triblock copolymer and halloysite nanotubes

Exequiel S. Rodríguez*, Victoria G. Falchi, Lucía Asaro, Ileana A. Zucchi, Roberto J.J. Williams

Institute of Materials Science and Technology (INTEMA), University of Mar del Plata and National Research Council (CONICET), Av. J. B. Justo 4302, 7600 Mar del Plata, Argentina

ARTICLE INFO

Keywords:
Halloysite nanotubes
Acrylic triblock copolymer
Epoxy composites
Thermal-mechanical properties
Fracture resistance

ABSTRACT

A hybrid epoxy composite was synthesized by adding halloysite nanotubes (HNTs) to an epoxy matrix toughened by an acrylic triblock copolymer (MAM). The morphology generated was composed of spherical MAM domains with sizes in the range of hundreds of nanometers and micron-size clusters of HNTs. The addition of HNTs produced an additional toughening effect with respect to the one generated by MAM. The critical stress intensity factor attained a maximum and then decreased due to the presence of defects generated when increasing the concentration of HNTs. An unexpected result was the decrease of the glass transition temperature produced when increasing the concentration of HNTs. This was ascribed to the different partition of starting monomers inside the cavities of nanotubes, generating a stoichiometric imbalance in the formulation.

1. Introduction

Due to their excellent thermal, mechanical and chemical properties, epoxy polymers are used in formulations of coatings, adhesives, matrices of composites and in advanced stimuli-responsive materials [1].For many applications, a variety of rigid particles alone or in a combination with rubbers or thermoplastics is used to obtain desired properties [2]. The role of halloysite, a biocompatible, abundant and cheap tubular clay material with structural formula $Al_2(OH)_4Si_2O_5.2H_2O$, as a modifier of epoxy networks has been reported in recent papers [3–10]. The tubular structure of halloysite results from the wrapping of the clay layers around onto themselves to form hollow cylinders. The halloysite nanotubes (HNTs) present an external surface composed of siloxane (Si-O-Si) groups and an internal surface containing aluminol (Al-OH) groups [11,12]. Dimensions of the inner and external diameters of HNTs depend on the clay source. Typical values range from 10 – 40 nm for the inner diameter and 30–100 nm for the external diameter, with typical lengths comprised between 0.2 and several μm. In the epoxy composites HNTs are dispersed as micron-size clusters with a size distribution depending on the functionalization of the surface and the processing conditions (in other polymeric matrices like PMMA, a dispersion of individual nanotubes has been reported [13]). In most cases, a significant increase in the fracture resistance was observed with the major energy dissipating mechanism assigned to the debonding, pull-out and breaking of individual HNTs.

The aim of the present study was to investigate the effect produced by the presence of both HNTs and a commercial acrylic triblock copolymer (MAM)in an epoxy composite. MAM was composed of a central poly(butyl acrylate) (PBuA) block and two terminal poly(methyl methacrylate) (PMMA) blocks. The addition of MAM produces a dispersion of elastomeric PBuA domains that toughens the epoxy matrix by cavitation and shear yielding mechanisms [14–17].

By taking a specific epoxy formulation modified by MAM as a reference material, we will discuss the effect of dispersing HNTs clusters on thermal-mechanical properties and fracture resistance of the hybrid composite.

2. Experimental

2.1. Materials

The diepoxy monomer was based on diglycidyl ether of bisphenol A (DGEBA, DER 383 Dow), with an epoxy equivalent weight of 182.6 g/eq as determined by titration (ASTM D1652, method B). A monoepoxy monomer based on C10 and C12 epoxidized alcohols (DLR001, Distraltec), was used as reactive diluent (RD). Its epoxy equivalent weight was 284 g/eq, also determined by titration (this value indicates the presence of a small fraction of the starting alcohols). The hardener was 4,4'-diamino-3,3'-dimethyl dicyclohexyl methane (3DCM,

* Corresponding author.
E-mail address: erodriguez@fi.mdp.edu.ar (E.S. Rodríguez).

https://doi.org/10.1016/j.coco.2018.12.010
Received 13 September 2018; Received in revised form 19 December 2018; Accepted 30 December 2018
Available online 31 December 2018

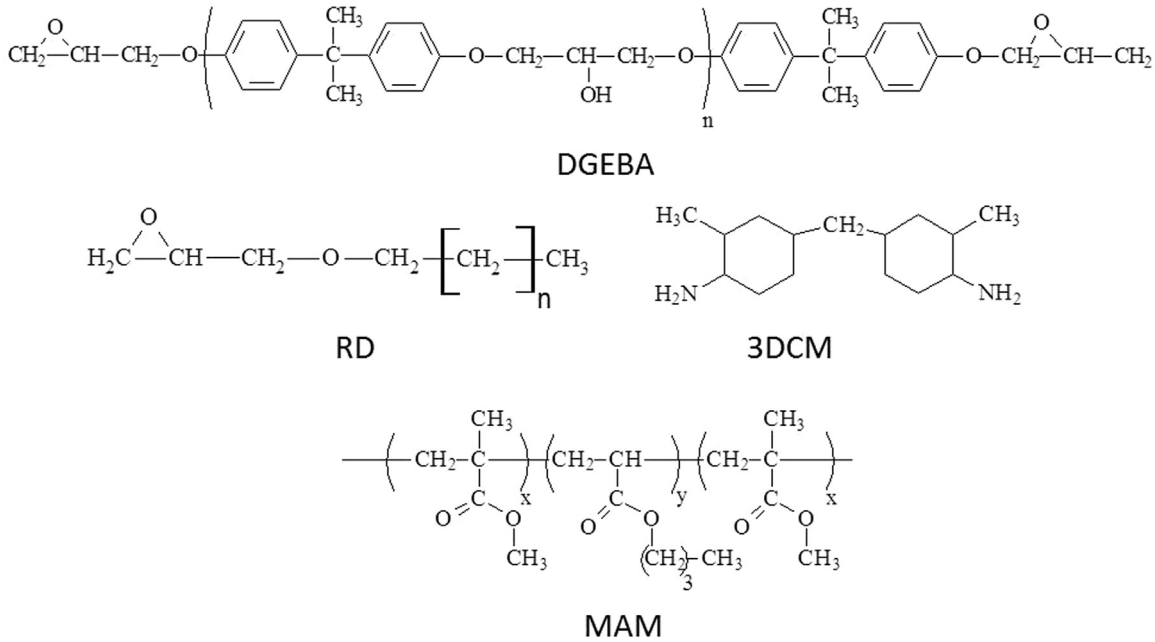

Fig. 1. Chemical structures of different components.

Ancamine 2049, Air Products, equivalent weight of 62.8 g/eq).The acrylic triblock copolymer (MAM, Nanostrength) was kindly supplied by Arkema (France).Its characterization was reported in a previous paper [17]. The number-average molar mass was M_n = 46 kg/mol and the mass-average molar mass was M_w = 66 kg/mol. The molar concentration of BuA was 40.2% and the one of MMA was 59.8%. Chemical structures of all these components are shown in Fig. 1.

Halloysite nanotubes (HNTs) were supplied by Aldrich. They were dried at 110 °C and used without any chemical modification. Their external diameters are in the range of 25 nm to 100 nm, their inner diameters range from 10 nm to 20 nm, and their lengths vary from 0.10 μm to 0.80 μm. (these values were obtained from TEM images, using Image Pro Plus).

2.2. Preparation of different samples

2.2.1. Synthesis of the MAM-modified epoxy used as reference

An amount of MAM equivalent to 5 wt % of the final mass was dispersed in DGEBA with mechanical stirring at 165 °C during 60 min. The transparent blend was cooled to room temperature and 20 wt % of RD with respect to DGEBA together with a stoichiometric amount of 3DCM were added with agitation. The blend was casted into an aluminum mold (20 × 15 × 0.5 cm), coated by a Teflon film. Cure was performed in a programmable convection oven using the following thermal cycle: 1 h at 60 °C, 1 h at 90 °C and 1 h at 120 °C.

2.2.2. Epoxy composites modified with MAM and HNTs

For these formulations, 1.5–5 wt % HNTs were added together with the RD after cooling the MAM-DGEBA blend to room temperature. The blend was transferred to a bath kept at 60 °C where vacuum was performed for 50 min to eliminate the air occluded inside the halloysite nanotubes. Then, ambient pressure was re-established and the blend was submitted to ultrasonication (Testlab, 25 °C, 160 W) for 10 min. After cooling, the stoichiometric amount of 3DCM was added with stirring and the cure was performed as described in the previous section.

2.3. Characterization

2.3.1. Viscosity

The viscosity was determined at 40 °C employing an Anton Paar rheometer (Physica-MCR-301), provided with a CTD 600 thermal chamber. A parallel-plate configuration was used at a rotation speed of 1 rpm.

2.3.2. Dynamic mechanical thermal analysis (DMTA)

Dynamic mechanical thermal analysis (DMTA) of different materials was performed employing a Q800 TA Instrument, in the three-point bending mode, at 1 Hz and 5 °C/min. Dimensions of samples were 12.5 × 65 × 5 mm, with a 50 mm spam.

2.3.3. Critical stress intensity factor (K_{IC})

The critical stress intensity factor, K_{IC}, was determined by three-point bending tests following the ASTM D5045 standard. Single-edge-notched beams with dimensions 4.5 × 9 × 40 mm, were tested using an Instron device with a cross-head speed of 0.2 mm/min. Reported values are the average of six valid results according to the ASTM standard.

2.3.4. Scanning electron microscopy (SEM)

Scanning electron microscopy (SEM) images were obtained using a Jeol JSM-6460LV device after coating fracture surfaces with a thin gold layer.

2.3.5. Transmission electron microscopy (TEM)

Transmission electron microscopy (TEM) images of ultrathin sections (about 60 nm thicknesses) were obtained employing a Jeol 100CX device. An LKB ultramicrotome was used to cut the specimens.

3. Results and discussion

3.1. Thermal-mechanical properties and fracture resistance of the MAM-modified epoxy

Fig. 2 shows a SEM image of the morphology produced in the MAM-modified epoxy network. The block copolymer is present as a distribution of spherical domains with sizes of several hundreds of nm. This morphology is generated as follows [16]. Initially (or early in the

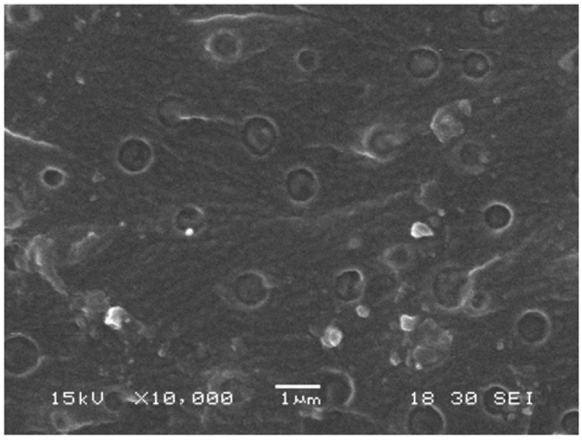

Fig. 2. SEM image of the morphology generated in the MAM-modified epoxy.

polymerization), MAM forms a micellar dispersion in the epoxy formulation, with micelles composed of rubbery PBuA cores stabilized with PMMA "hairs" that are solubilized in the epoxy. However, as polymerization of the epoxy takes place, PMMA becomes insoluble [18] generating the spherical domains by a reaction-induced phase separation process [19].The SEM image clearly shows cavitation inside dispersed domains that promotes shear yielding of the epoxy matrix. The critical stress intensity factor was K_{IC} = 0.99 MPa m$^{0.5}$, compared with K_{IC} = 0.60 MPa m$^{0.5}$ for the unmodified epoxy.

Fig. 3 compares DMTA results for the unmodified epoxy and MAM-modified epoxy. The most significant result is the increase in the alpha-relaxation temperature observed (temperature of the maximum in tan δ, related to the glass transition temperature) in the modified sample. It increased from 101 °C for the unmodified epoxy to 109 °C for the MAM-modified sample. This effect which has been previously reported for a different formulation [17], is contrary to the one observed with typical rubbers such as CTBN. The lack of plasticization is simply due to the fact that there is no residual PBuA remaining dissolved in the epoxy matrix. The increase in the alpha-relaxation may be ascribed to the interlocking of PMMA blocks and the epoxy matrix at the surface of dispersed domains. This could also explain the slightly increase in the rubbery modulus. Therefore, addition of MAM has two positive effects; it produces a significant increase in toughness and a slight increase in the glass transition temperature. The storage modulus is only slightly affected. At 35 °C, it decreases from 2.53 GPa to 2.46 GPa.

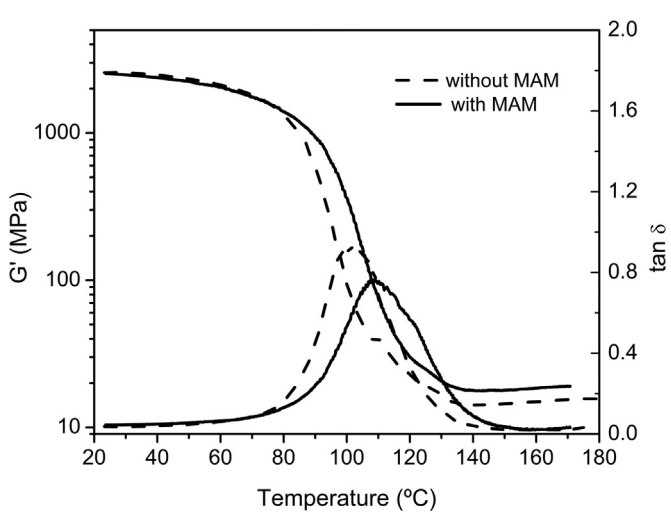

Fig. 3. Storage modulus (*G'*) and loss factor (tan δ) for unmodified and MAM-modified epoxy.

3.2. Hybrid epoxy composites containing HNTs

The range of convenient HNT concentrations was limited by the increase in viscosity. For example, at processing conditions (40 °C), MAM-modified epoxy had a viscosity of 483 mPa s. Viscosities of formulations containing 1.5 and 3 wt % HNT were 560 mPa s and 650 mPa;s. This was near the maximum limit acceptable for common processing techniques. Clusters of HNTs with a broad distribution of sizes were uniformly dispersed in the hybrid material. Fig. 4a shows a SEM image of the hybrid epoxy composite containing 3 wt %HNTs. A large cluster of HNTs indicated by an arrow is observed. TEM images of another cluster are shown in Fig. 4b. The black bar in the left image indicates 0.2 μm while the one in the image at the right corresponds to 50 nm. In the image with the lowest magnification, white domains are those of the block copolymer. In the image with the largest magnification, individual nanotubes surrounded by the epoxy matrix are observed.

An additional effect on the fracture resistance was produced by the presence of HNTs clusters. The critical stress intensity factor increased from K_{IC} = 0.99 MPa m$^{0.5}$ (no HNTs) to 1.20 MPa m$^{0.5}$ (1.5 wt % HNTs) and 1.36 MPa m$^{0.5}$ (3 wt % HNTs). However, it decreased to 1.10 MPa m$^{0.5}$ for 5 wt % HNTs. The energy dissipation mechanisms occurring inside clusters add to the conventional cavitation-matrix shear yielding mechanism produced by the dispersion of MAM domains. However, addition of large amounts of HNTs increases the viscosity of the starting formulation and generates defects (e.g., small air bubbles) whose presence decreases the fracture resistance. The toughening potential of using both additives is demonstrated by the fact that K_{IC} for 1.5 wt % HNTs without MAM was only 0.62 MPa m$^{0.5}$.

Fig. 5 shows DMTA results for the hybrid epoxy composites containing different amounts of HNTs. Glassy and rubbery moduli were practically the same. However, a decreasing trend of the alpha-relaxation temperature with the amount of HNT was observed (108.6 °C, 107.9 °C, 105.2 °C and 102.5 °C for samples with 0, 1.5, 3 and 5 wt % HNT). A possible explanation of this effect might be the presence of a partitioning effect of the epoxy monomers and the diamine hardener inside the HNT. As the internal surface is electrophilic due to the presence of aluminol groups, the diamine can increase its relative concentration inside the HNT producing a slight stoichiometric imbalance in the matrix that generates the observed decrease of the glass transition temperature.

4. Conclusions

The addition of HNTs to a rubber-toughened epoxy matrix produced an additional toughening effect ascribed to the energy dissipation mechanisms present inside HNTs clusters (debonding, pull-out and breaking of individual nanotubes). However, the existence of an optimum amount was observed (about 3 wt % in the present case). This was ascribed to the introduction of defects such as air bubbles in samples containing large mass fractions of HNTs. A secondary effect produced by the addition of HNTs was the decrease of the glass transition temperature. This was ascribed to the partition of the starting monomers inside the cavities of HNTs generating a stoichiometric imbalance in the formulation.

Acknowledgement

The authors acknowledge the financial support of the University of Mar del Plata, the National Research Council (CONICET) and the National Agency for the Promotion of Science and Technology (ANPCyT).

Declarations of interest

None.

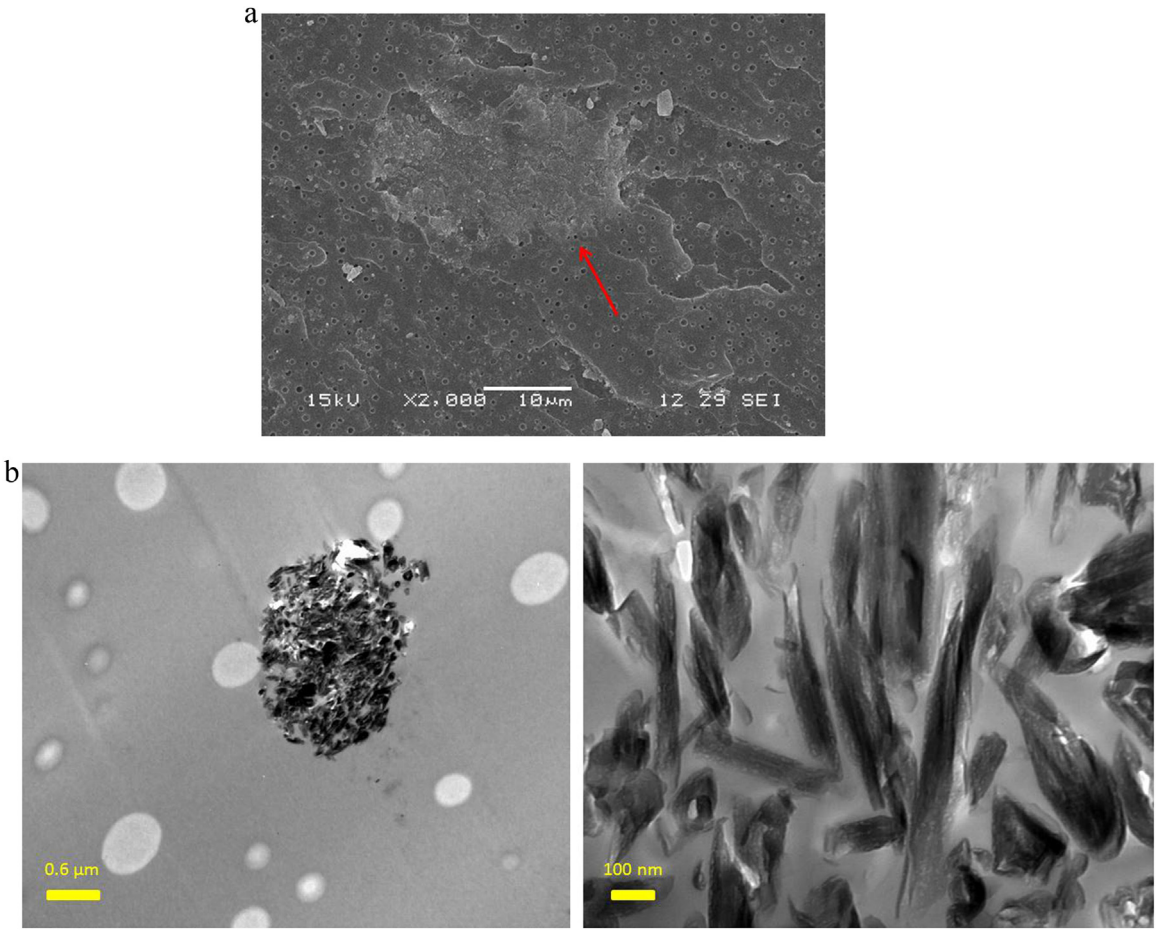

Fig. 4. a.SEM image of the hybrid epoxy containing 3 wt % HNTs (the arrow indicates the presence of a large cluster of HNTs of several tenths of microns in size). **b.**TEM images with different magnifications of the hybrid epoxy containing3 wt % HNTs.

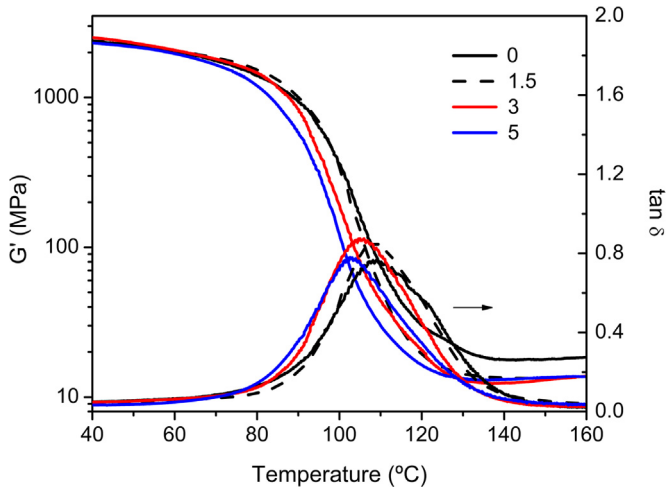

Fig. 5. Storage modulus (*G'*) and loss factor (tan *δ*) for the hybrid epoxy composites containing 0, 1.5, 3 and 5 wt % HNTs.

References

[1] J.P. Pascault, R.J.J. Williams (Eds.), Epoxy Polymers: New Materials and Innovations, Wiley-VCH, Weinheim, 2010(ISBN: 978-3-527-62871-1).

[2] P.P. Vijayan, D. Puglia, M.A.S.A. Al Maadeed, J.M. Kenny, S. Thomas, Elastomer/thermoplastic modified epoxy nanocomposites: the hybrid effect of micro and nanoscale, Mater. Sci. Eng. R 116 (2017) 1–29, https://doi.org/10.1016/j.mser.2017.03.001.

[3] Y. Ye, H. Chen, J. Wu, L. Ye, High impact strength epoxy nanocomposites with natural nanotubes, Polymer 48 (21) (2007) 6426–6433, https://doi.org/10.1016/j.polymer.2007.08.035.

[4] S. Deng, J. Zhang, Y. Ye, J. Wu, Toughening epoxies with halloysite nanotubes, Polymer 49 (23) (2008) 5119–5127, https://doi.org/10.1016/j.polymer.2008.09.027.

[5] S. Deng, J. Zhang, L. Ye, Halloysite-epoxy nanocomposites with improved particle dispersion through ball mill homogenization and chemical treatments, Compos. Sci. Technol. 69 (14) (2009) 2497–2505, https://doi.org/10.1016/j.compscitech.2009.07.001.

[6] J. Zhang, Z. Jia, D. Jia, D. Zhang, A. Zhang, Chemical functionalization for improving dispersion and interfacial bonding of halloysite nanotubes in epoxy nanocomposites, High. Perform. Polym. 26 (7) (2014) 734–743, https://doi.org/10.1177/0954008314528226.

[7] V. Vahedi, P. Pasbakhsh, Instrumented impact properties and fracture behavior of epoxy/modified halloysitenanocomposites, Polym. Test. 39 (2014) 101–114, https://doi.org/10.1016/j.polymertesting.2014.07.017.

[8] V. Vahedi, P. Pasbakhsh, S.P. Chai, Toward high performance epoxy/halloysite-nanocomposites: new insights based on rheological, curing, and impact properties, Mater. Des. 68 (2015) 42–53, https://doi.org/10.1016/j.matdes.2014.12.010.

[9] P. Sun, G. Liu, D. Lv, X. Dong, J. Wu, D. Wang, Simultaneous improvement in strength, toughness, and thermal stability of epoxy/halloysite nanotubes composites by interfacial modification, J. Appl. Polym. Sci. 133 (13) (2016) 43249, https://doi.org/10.1002/app.43249.

[10] J. Zhang, S. Deng, Y. Wang, L. Ye, Role of rigid nanoparticles and CTBN rubber in the toughening of epoxies with different cross-link densities, Compos A80 (2016) 82–94, https://doi.org/10.1016/j.compositesa.2015.10.017.

[11] P. Yuan, P.D. Southon, Z. Liu, M.E.R. Green, J.M. Hook, S.J. Antill, C.J. Kepert, Functionalization of halloysite clay nanotubes by grafting with □-aminopropyltriethoxysilane, J. Phys. Chem. C 112 (40) (2008) 15742–15751, https://doi.org/10.1021/jp805657t.

[12] M. Liu, Z. Jia, D. Jia, C. Zhou, Recent advance in research on halloysitenanotubes-polymer nanocomposite, Prog. Polym. Sci 39 (8) (2014) 1498–1525, https://doi.org/10.1016/j.progpolymsci.2014.04.004.

[13] K. Pal, Effect of different nanofillers on mechanical and dynamic behavior of PMMA based nanocomposites, Compos. Commun. 1 (2016) 25–28, https://doi.org/10.1016/j.coco.2016.08.001.

[14] R.M. Hydro, R.A. Pearson, Epoxies toughened with triblock copolymers, J. Polym.

Sci. B Polym. Phys. 45 (8) (2007) 1470–1481, https://doi.org/10.1002/polb.21166.
[15] H. Kishi, Y. Kunimitsu, J. Imade, S. Oshita, Y. Morishita, M. Asada, Nano-phase structures and mechanical properties of epoxy acryl/triblock copolymer alloys, Polymer 52 (3) (2011) 760–768, https://doi.org/10.1016/j.polymer.2010.12.025.
[16] M.T. Bashar, U. Sundararaj, P. Mertiny, Morphology and mechanical properties of nanostructured acrylic tri-block-copolymer modified epoxy, Polym. Eng. Sci. 54 (5) (2014) 1047–1055, https://doi.org/10.1002/pen.23648.
[17] L.M. Sáiz, A.B. Orofino, E.S. Rodríguez, I.A. Zucchi, R.J.J. Williams, Epoxy formulation including an acrylic triblock copolymer adapted for use in filament winding, Polym. Eng. Sci. 56 (10) (2016) 1153–1159, https://doi.org/10.1002/pen.24348.
[18] C.M. Gómez, C.B. Bucknall, Blends of poly(methyl methacrylate) with epoxy resin and an aliphatic amine hardener, Polymer 34 (10) (1993) 2111–2117, https://doi.org/10.1016/0032-3861(93)90737-U.
[19] R.J.J. Williams, B.A. Rozenberg, J.P. Pascault, Reaction-induced phase separation in modified thermosetting polymers, Adv. Polym. Sci. 128 (1997) 95–156, https://doi.org/10.1007/3-540-61218-1_7.